



Multimodal image fusion with SIMS: Preprocessing with image registration

Jay Gage Tarolli, Anna Bloom, and Nicholas Winograd

Citation: *Biointerphases* **11**, 02A311 (2016); doi: 10.1116/1.4939892

View online: <http://dx.doi.org/10.1116/1.4939892>

View Table of Contents: <http://scitation.aip.org/content/avs/journal/bip/11/2?ver=pdfcov>

Published by the AVS: Science & Technology of Materials, Interfaces, and Processing

Articles you may be interested in

[The use of atlas registration and graph cuts for prostate segmentation in magnetic resonance images](#)

Med. Phys. **42**, 1614 (2015); 10.1118/1.4914379

[Multiattribute probabilistic prostate elastic registration \(MAPPER\): Application to fusion of ultrasound and magnetic resonance imaging](#)

Med. Phys. **42**, 1153 (2015); 10.1118/1.4905104

[Fully automated segmentation of cartilage from the MR images of knee using a multi-atlas and local structural analysis method](#)

Med. Phys. **41**, 092303 (2014); 10.1118/1.4893533

[Automatic segmentation of head and neck CT images for radiotherapy treatment planning using multiple atlases, statistical appearance models, and geodesic active contours](#)

Med. Phys. **41**, 051910 (2014); 10.1118/1.4871623

[Feature-based multibody rigid registration of CT and ultrasound images of lumbar spine](#)

Med. Phys. **39**, 3154 (2012); 10.1118/1.4711753

Multimodal image fusion with SIMS: Preprocessing with image registration

Jay Gage Tarolli,^{a)} Anna Bloom, and Nicholas Winograd

Department of Chemistry, The Pennsylvania State University, 104 Chemistry Building, University Park, Pennsylvania 16802

(Received 2 November 2015; accepted 4 January 2016; published 14 January 2016)

In order to utilize complementary imaging techniques to supply higher resolution data for fusion with secondary ion mass spectrometry (SIMS) chemical images, there are a number of aspects that, if not given proper consideration, could produce results which are easy to misinterpret. One of the most critical aspects is that the two input images must be of the same exact analysis area. With the desire to explore new higher resolution data sources that exists outside of the mass spectrometer, this requirement becomes even more important. To ensure that two input images are of the same region, an implementation of the insight segmentation and registration toolkit (ITK) was developed to act as a preprocessing step before performing image fusion. This implementation of ITK allows for several degrees of movement between two input images to be accounted for, including translation, rotation, and scale transforms. First, the implementation was confirmed to accurately register two multimodal images by supplying a known transform. Once validated, two model systems, a copper mesh grid and a group of RAW 264.7 cells, were used to demonstrate the use of the ITK implementation to register a SIMS image with a microscopy image for the purpose of performing image fusion. © 2016 American Vacuum Society. [<http://dx.doi.org/10.1116/1.4939892>]

I. INTRODUCTION

Image fusion has gained traction as a method to improve the image quality of secondary ion mass spectrometry (SIMS) images by combining the data with other sources of high resolution information. Previously used across disciplines that include medical imaging,^{1,2} satellite imaging,^{3–5} and remote sensing,^{6–8} image fusion combines the data from two or more images, or sensors, to create an output image containing more information than any of the input images alone.^{9,10} While other methods exist to improve SIMS images by multivariate analysis^{11,12} and other statistical approaches,^{13,14} these images, especially when involving complex, biological systems, often suffer from an inherent lack of information available to analyze. Image fusion works to augment SIMS data with information acquired from complementary analytical techniques with the output image presenting chemical information with greater resolution and clarity.

When performing image fusion, there are a number of aspects of the process that, if careful attention is not given, can result in color artifacts or otherwise inaccurate results. This could include the introduction of new information that distorts or adds artificial shadowing, such as topographical and morphological information. The addition of morphological information to a SIMS image has been shown to improve the analysis of *Botryococcus braunii* algal colonies,¹⁵ as long as it is not misinterpreted. Another consideration is the appearance of gray pixels when fusing through pan-sharpening, which is the result of signal present at a given pixel in the higher resolution, panchromatic image, but not present in the multispectral SIMS image. While gray pixels could be considered artifacts, it was previously shown that

they may still represent valuable chemical information, such as the distribution of lipid molecules in cells, just with less chemical specificity.¹⁶ Other aspects which need to be addressed include the relative intensity scales between the input images and ensuring that the input images are registered prior to fusion.¹⁷

For image fusion to become a more widespread data processing technique for SIMS, it must be ensured that artifacts stemming from misaligned input images will not be introduced. These color artifacts are avoided by incorporating image registration, a necessary preprocessing step for performing image fusion.^{8,18,19} Image registration seeks to determine the transform that maps one image, called the moving image, to the image space of another image, the fixed image, to the highest degree. This is accomplished by repeatedly transforming the moving image and determining the degree of similarity between it and the fixed image. The degree of similarity between the two images can be measured in terms of intensity values of pixels in the images,^{20–22} a set of control points that define corresponding locations that represent the same point in physical space,²³ and objects and features that are common to both images.^{18,24} For the multimodal registration with SIMS images presented in this work, intensity based image registration is sufficient, as the input images will have similar intensity patterns. Intensity based registration is chosen over control point and region methods since SIMS images are often noisy, and thus, may not have well defined features. This would make automatic control point and feature detection difficult and unreliable, while manual identification of features by a user would introduce uncertainty.

Because registration of images is not a novel problem to be addressed, tools exist for implementing image registration to individual applications. For the work presented here, the

^{a)}Electronic mail: jgt143@psu.edu

insight segmentation and registration toolkit (ITK) was chosen to provide the framework for the image registration since most of the underlying calculations and methods have already been developed and extensively tested. The end result of registration is two images which are, with confidence, of the same exact area. This means that when applying image fusion to the images, it can be said with certainty that each pair of pixels from the input images being compared are of the same chemical environment. With that, the resulting fused image preserves the chemical integrity of the data while supplementing it with complementary, higher resolution information.

Registration of two images is a process that requires careful attention to the task being performed for a number of reasons. In order to register images with the procedure outlined in this work, there must be visible features within the system being analyzed that are present in both images. Otherwise, the similarity metric would not be able to quantify the correlation between the two images. Ideally, these features would be prominent and well defined in both images; however, as the examples in this paper will show, multimodal registration is possible by using a Mattes mutual information metric. If there is little or no commonality between the images, then the pair will not be registered with any degree of accuracy.

In order to utilize image registration as a preprocessing step for multimodal image fusion with SIMS images and an image acquired with a higher resolution data source located outside of the mass spectrometer, the implementation of the ITK toolkit must first be verified to ensure that the correct registration is obtained. A copper mesh system is imaged using both SIMS and secondary electron microscopy (SEM) where the two images were acquired with a known offset. The results from the registration procedure are compared to the known offset to confirm that the correct transform has been determined by the ITK implementation. Next, a fluorescent dye is spin cast onto a slide to form a uniform thin film and is then covered with a copper mesh grid to block the film in a predictable pattern. In this case, the fluorescence microscopy image has a higher spatial resolution than the SIMS image. Fusing the fluorescence microscopy image with the chemical image of the fluorescent dye combines both the chemical information from the SIMS image and the high spatial resolution afforded by the microscopy image. This sample serves as an excellent model system for the experiment because there are only two chemical components, the dye and the copper grid. When fusing the chemical signal of the dye with the fluorescence signal, the same exact chemistry is being directly compared, as all fluorescent signal is due to the fluorescent dye.

The third system seeks to demonstrate the registration and fusion process when applied to a more complex, biological sample. RAW 264.7 cells are first imaged with optical microscopy, which, again, offers greater spatial resolution than a corresponding SIMS image. The microscopy image is then registered and fused with the chemical signals of phosphocholine, a major lipid component of the cell membrane, and adenine, a prominent component of the nucleus. The

resulting fused image aims to improve the resolution of the chemical image to better visualize the distribution of the cell membrane and nucleus. An interesting consequence of the proper registration of the microscopy and SIMS images of RAW 264.7 cells highlights another limitation of combining multimodal images. In this experiment, the chemical distributions appear to shift throughout a SIMS 3D depth profile, which is due to nonuniform sputtering through heterogeneous samples.

II. EXPERIMENT

A. SEM–SIMS image pair

A pair of images with a known offset was acquired to validate the registration algorithm that was implemented. To do this, the Bio-ToF SIMS imaging mass spectrometer described elsewhere,²⁵ equipped with a 40 keV C₆₀ primary ion source (Ionoptika, Ltd., Southampton, UK) mounted 40° off normal, was used to acquire a pair of images of a copper mesh grid, one image being a SIMS image and the other an SEM image. The raster control unit on the instrument has the capability to alter the analysis area on the sample in order to generate two images with a known offset. The analysis area of the primary beam can be deflected, or shifted in the x- and y-dimensions to generate a translation transform. In addition, the analysis area can be rotated around the center of the area in order to create a rotation transform. Finally, the field of view, or the size of the raster area, can be changed to produce a scale transform. Two or more of these transforms can be applied at the same time to generate complex transforms to validate the registration implementation.

B. Fluorescence microscopy–SIMS image pair

To create a system with distinct fluorescently active regions, a solution of the fluorescent dye, fluorescein isothiocyanate (FITC) (Fisher Scientific, Pittsburgh, PA), was prepared by dissolving 0.1 mg of the dye in 0.2 ml anhydrous toluene. The resulting solution was spin cast onto a 0.5 × 0.5 cm indium tin oxide (ITO) coated glass shard. A 400 mesh copper grid was affixed with silver paste on top of the fluorescent film to block the dye in a regular and predictable pattern.

Fluorescence microscopy images of a characteristic feature on the grid, such as a letter or number, were acquired. A 40× magnification was used to produce images with a field of view of approximately 120 μm. The resulting images were relief images of the grid, which blocked the dye emission from reaching the camera.

Time-of-flight secondary ion mass spectrometry (ToF-SIMS) analysis was performed with the Bio-ToF mass spectrometer using 200 shots/pixel to obtain spectra that were 256 × 256 pixels with a field of view of 215 × 215 μm. Mass spectral images were then generated using *m/z* 391, which is the [M + H]⁺ signal of the FITC dye.

C. Optical microscopy–SIMS image pair

RAW 264.7 cells, macrophagelike cells derived from tumors induced in mice by the Abelson murine leukemia virus, were maintained in Dulbecco's modified Eagle's medium at 37°C and 5% CO₂. After rinsing with Dulbecco's phosphate buffered saline (DPBS), cells were detached from culture flasks using a cell scraper and cultured onto ITO. These chips had been cleaned by sonication in chloroform, acetone, methanol, and purified water. RAW 264.7 cells were allowed to grow for 24 h.

After the 24 h incubation period, the cell covered ITO chips were removed from media. Cells were chemically fixed using formalin (2.5% glutaraldehyde in 0.1 M sodium cacodylate) for 15 min. After fixation, cells were washed five times in DPBS to remove excess fixing solution and then three times in Millipore water, followed by 0.015 M ammonium formate (pH 7.3). Ammonium formate was used to minimize variation from accepted cellular preparation methods which utilize this solution to remove residual salts. The samples were allowed to air dry for 10 min prior to insertion in the ToF-SIMS.

Score marks were scratched into the surface of the ITO coated glass substrate in distinct patterns before cell fixation to create points of reference for matching up areas between images. Optical microscope images were obtained of several areas near score marks at 20× magnification with an approximately 200 × 200 μm field of view. The images were converted to grayscale, and the color was inverted so that the cells appear bright and the background becomes black, to match the direction of the intensity scale of SIMS images.

SIMS images were then acquired using the J105 3D Chemical Imager (Ionoptika, Ltd., Southampton, UK), equipped with a 40 keV C₆₀ primary ion beam. Secondary electron images were taken to locate a region for which an optical image had been already obtained, matching score marks and the position of cells. Once a suitable region was found, a 3D depth profile, where each image layer was 256 × 256 pixels with a field of view of 100 × 100 μm, was obtained. A primary ion dose of 4 × 10¹³ ions/cm² was used to acquire 15 layers.

D. Image registration and using ITK

Before fusing two images, the pair must first be registered to ensure the regions in each image are exactly the same. In

order to register a pair of images, ITK, which is an open source set of libraries for image analysis and, specifically, image registration,²⁶ was implemented into a custom data analysis software application. The implementation of the ITK libraries was developed to be suitable for registering a SIMS image with a higher resolution image for the purpose of applying image fusion. Considerations that went into the design include support for multimodality image pairs, which would be necessary for registering a SIMS image with an optical or fluorescence microscopy image, and the desire to preserve as much chemical information as possible. The ITK library provides the software support for the majority of the pipeline, such as classes describing different transforms, optimizers to quickly and efficiently determine the optimal transform, and metrics for quantifying the similarity between the two images. A complete guide for using ITK to perform image registration can be found in the ITK documentation (<http://itk.org/ITK/resources/software.html>), and a block diagram of the registration process, which is described in detail next, is shown in Fig. 1.

To register a pair of images, they must be of the same resolution. If necessary, the lower resolution image is upsampled to match the resolution of the other image using bilinear interpolation. Two copies of a pair of unregistered images are then loaded from disk; a color image is first loaded to memory and then a grayscale copy of the image is created and used for the registration procedure. During the registration procedure, a metric will compare the intensities between the two images, and, as such, a single grayscale intensity value is necessary. A curvature flow smoothing filter was applied to the images before registration to remove noise that is often present in SIMS images. Isointensity contours in an image are used to perform edge-preserving smoothing, similar to that of anisotropic diffusion smoothing.²⁷

For registering a SIMS image with an image acquired using a different modality, three degrees of transform need to be accounted for: translation, rotation, and scale. Since the image pair is being acquired with two separate sets of instrumentation, the position and field of views will be different between the two images. In addition, depending on the physical set up of the instruments, the two images are likely to be rotated to some degree about a point in the image. Therefore, a transform which will account for all three modes of transformation needs to be used for registration, which, in ITK, is called a centered similarity transform. Additional types of

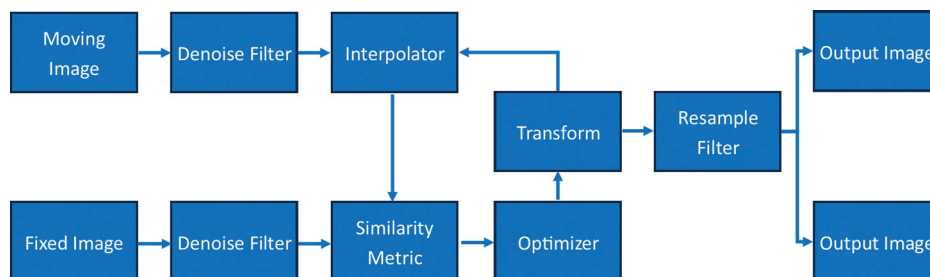


FIG. 1. Flow diagram of the registration process with key components.

distortion, such as skewing, may be possible, but were not deemed to be necessary to transform optical microscopy images with SIMS images given the instrumentation used.

An initial transform specified by the user is then applied to the moving image using an interpolator to calculate the intensity values that fall between pixels in the original image and a metric is used to quantify the similarity between the transformed and the fixed images. For registration of the SEM–SIMS image pair and the optical–SIMS image pair, multimodal registration was necessary to account for the significant difference in relative intensity scales between the two images. In such a case, a Mattes mutual information metric was used to determine the degree of similarity between the two images. Mutual information metrics utilize information theory and are based on the entropy difference between two images. Entropy, here, is a measure of uncertainty in the probability distribution of grayscale intensity values throughout an image.²⁸ The difference in entropy between two images is the measure of mutual information, and is not limited by the images being acquired using the same modality.²⁷ However, for registration of the fluorescence–SIMS image pair, the images were similar enough in relative intensity that this was not necessary, and a more basic mean squares metric was used to quantify the similarity. The mean squares metric determines the average difference between intensities at each pair of corresponding pixels in two images and, thus, is a simpler and more computationally efficient method appropriate for images acquired with similar relative intensity scales.²⁷

The result of the similarity metric is passed to an optimizer, which determines the next set of parameters (translation, rotation, and scale) to transform the moving image, taking into account previous transforms attempted and the directions of movement that increased the metric. A gradient descent optimizer is used to seek a maximum in the similarity between the transformed and fixed images, which will indicate that the registration process has been completed. Steps are taken by the optimizer to move toward the maximum and away from local minima in order to reach convergence. The next transform is applied to the moving image, the similarity is determined, passed to the optimizer, and the process is repeated until the maximum similarity has been determined.

Once the optimal transform has been determined, the final step is to resample the original color images to produce a pair of images that are now registered. The resample filter takes the final transform, which resulted in the maximum correlation between the moving and fixed images, and applies it to the input moving image so that it is now in the same image space as the fixed image. A final step is performed to remove pixels from the fixed image, which correspond to pixels in the moving image that originated outside of the original image space, and were therefore not measured during analysis. This ensures that only information that is present in both images is retained, an important aspect since these registered images are being used for image fusion. Finally, the registered images are saved to disk.

Unfortunately, registering images with the above components is still not a straightforward, perfect process. Several

aspects of the registration process are tunable, and in order to obtain reliable results, these must be monitored and optimized. In addition, there is a tradeoff between accuracy of registration and the speed of the registration process. Unfortunately, the optimal parameters and the middle ground between accuracy and efficiency are usually experiment specific and must be addressed on a case-by-case basis.

In order to successfully register two images, the maximum of the metric value must be found by the optimizer. When the optimizer calculates a local maximum, it breaks and the registration process completes with that transform. Unfortunately, the optimizer is susceptible to becoming trapped in local maxima that are not the true maximum, resulting in images that are not truly registered. One approach that has success in overcoming this problem is to input initial transform guesses. A user interface was constructed to allow the user to manually translate, rotate, and scale the moving image with respect to the fixed image. The parameters generated from this are then supplied to the registration process and used to construct the first transform passed to the optimizer. This allows the human eye to align the two images before performing registration, which significantly reduces room for error in the registration process. This also speeds up the registration process, as the optimizer is beginning at a transform that is already fairly close to convergence.

Another approach for avoiding the optimizer becoming trapped by local maxima is to adjust the step lengths taken between transforms. The registration framework allows for a maximum and a minimum step length to be specified for the optimizer, which restricts how far the optimizer will jump from one transform to the next. The larger the steps the optimizer is taking between transforms, the quicker the registration process will complete. However, if the step sizes are too large, the optimizer is likely to miss transforms, which will more accurately steer the direction of the transforms. Using too small of a step length will result in a registration attempt taking too long. A good tradeoff between accuracy and speed for registering SIMS images is a maximum step length of 0.01 and a minimum step length of 0.001 for most experiments.

If prominent features are visible to the user in both images, another strategy for avoiding local maxima is to restrict the area of the fixed image, which is compared to the moving image with the metric. Defining a region of interest (ROI) aims to reduce ambiguous signal, such as regularly repeating grid lines, which could lead to the optimizer becoming trapped by a local maximum. In addition, if a significant amount of noise is present, defining the ROI where noise is not present, or insignificant, would increase the accuracy of the registration. Finally, the speed of the registration increases as the size of the ROI decreases with respect to the full size of the fixed image. The registration framework allows a ROI to be defined for the fixed image only, and not the moving image. However, it was found that defining as small of an ROI as possible around features that are distinct, prominent, and specific greatly improved the accuracy of the registration result.

For multimodal registration, two additional parameters are introduced, which affect the accuracy and speed of image registration. As described earlier, multimodal registration involves a different metric that compares mutual information between the moving and fixed images. The metric analyzes the histograms of each image and calculates an entropy difference. Therefore, the registration framework allows for the number of histogram bins to be set, as well as the number of pixels in the images to sample and place into the histogram bins. As would be expected, the larger the number of samples used, the better the registration result, yet the longer the duration of the process. For the experiments in this work, 50 histogram bins and 10 000 pixel samples produced a sufficient tradeoff between accuracy and efficiency. However, setting the metric to analyze all pixels did not significantly slow down the registration process.

E. Image fusion

After the input images had been successfully registered, image fusion was applied to the image pair. The high resolution image was used as the panchromatic image and the SIMS image was used as the multispectral image to perform image fusion via pan-sharpening. An adapted pan-sharpening algorithm, which has been detailed and applied previously,^{15,16} was used to generate the fused images.

III. RESULTS AND DISCUSSION

A. Confirmation with a known transform

Before applying image registration to ToF-SIMS data, it must first be confirmed whether the implementation performs as expected. Mainly, it must be determined if the algorithm produces the correct transform which will register a moving image with a fixed image. To validate the registration process, a pair of SEM images of a copper mesh grid was acquired with a known rotation and scale between the two images to create a centered similarity transform.

The moving image is an SEM image while the fixed image is a SIMS image of copper (m/z 63), shown in Figs. 2(b) and 2(a), respectively. Both images are 256×256 pixels. For the fixed image (SIMS), a $515 \times 515 \mu\text{m}$ field of view was used, while a $1023 \times 1023 \mu\text{m}$ field of view was used for the moving image (SEM). This created an intentional scaling of the images by a factor of 0.503. The ITK framework uses the size of the fixed image divided by the moving image when defining scale. In addition to the scale, a rotation of -15° around the center of the raster area was also applied. For registration in this experiment, denoising was applied since noise was present in between the grid lines in the SIMS image and a ROI was defined around the letters "O" and "V" in the fixed image. The registered images are shown in Figs. 2(c) and 2(d). The results of registration are shown in Table I, along with the parameters of the known

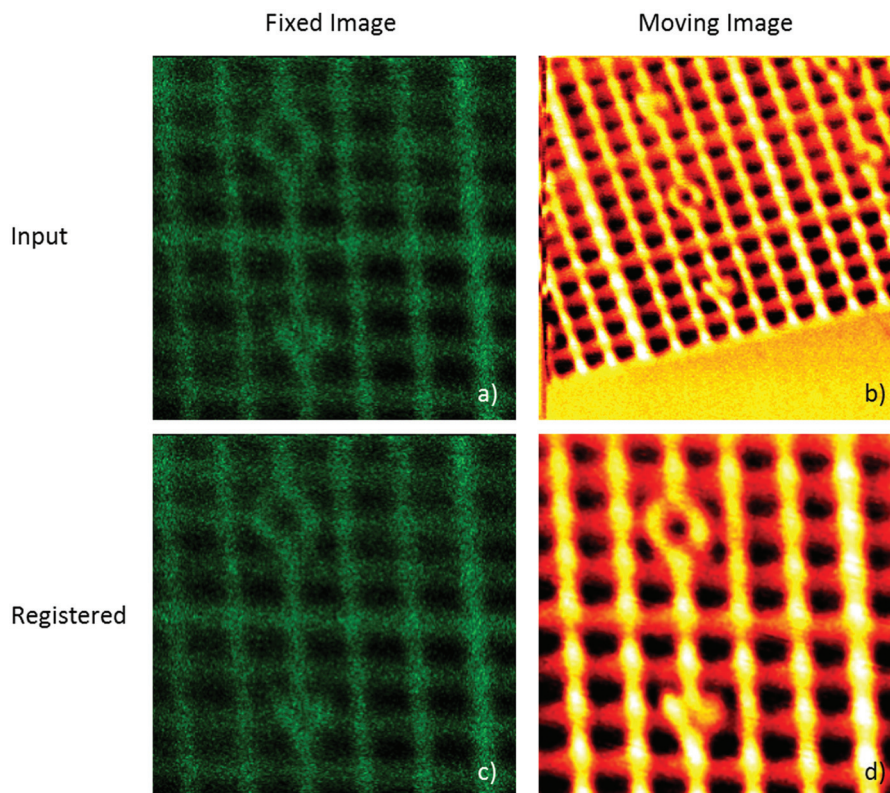


FIG. 2. Example of a pair of images offset by a known scale rotation: (a) fixed SIMS image (green: m/z 63) with no rotation and a field of view of $515 \times 515 \mu\text{m}$; (b) moving SEM image intentionally rotated 15° around the image center and a field of view of $1023 \times 1023 \mu\text{m}$; (c) fixed image after registration and resampling; and (d) moving image after registration and resampling. All images are 256×256 pixels.

TABLE I. Transform parameters of the known transform supplied to offset the images in Fig. 2 and the resulting transform that was calculated by the ITK registration algorithm.

	Supplied	Calculated
Translation	(0.0, 0.0)	(−1.49, 0.524)
Rotation	−15.0°	−14.6°
Scale	0.503	0.498

transform that was supplied. The resulting scale and angle of rotation determined by the registration procedure are well in agreement with the supplied offsets. This validates that the method is able to properly register two multimodal images, specifically where one is a SIMS image. A minimal translation was calculated (−1.49 pixels, 0.524 pixels), even though no translation was specified. However, this is likely due to the exact location of the rotation center being located between pixels. Similar results were obtained for pairs of images that contained only one of the transforms (translation, rotation, and scale), as well as translation and rotation combined. Please see supplementary material for examples of these experiments in Figs. SI-1 and SI-2.²⁹

B. Registration and fusion of fluorescence–SIMS image pair of copper grid

To demonstrate the capabilities of the ITK registration framework as a preprocessing step for image fusion, an image pair was acquired of a fluorescent dye thin film covered with a copper mesh grid. This system was designed to fuse fluorescence information in the form of emitted light in a fluorescence microscopy image, and the chemical information of the fluorescent dye in a SIMS image. Since the microscope used to acquire the fluorescence image shines light from below to excite the dye and the camera is positioned above, what will be seen in the image is the dye fluorescing behind the grid. Similarly, when analyzed with SIMS, the dye signal at m/z 391 that is used to create the image will be present in the areas between grid lines.

A pair of images was acquired, focusing on the letter “R” in the grid, and are shown in Fig. 3. It is clearly seen that the input images in Figs. 3(a) and 3(b) contain the same physical feature, but are not well aligned. To correct this, the images were registered using a centered similarity transform to account for the different fields of view, as well as the rotation and translation offsets between the two images. The results of the registration procedure are shown in Table II, which were obtained after 243 iterations. From visual inspection, the images in Figs. 3(c) and 3(d) appear registered.

Before registering the images, the moving image—in this case, the fluorescence image in Fig. 3(b)—was manually scaled, rotated, and translated with respect to the fixed image to generate an initial estimate of the transform to supply as a starting point for the registration process. The initial estimate produced an angle of 75° and a scale of 1.88, which are both very close to the registration results. In addition, the scale returned, 2.02, agrees with the fields of view of the two

images, which is known to be $215 \times 215 \mu\text{m}$ for the SIMS image and approximately $120 \times 120 \mu\text{m}$ for the fluorescence image. Given that the transform results agree with the estimated transform, the ratio of fields of view agree with the resulting scale, and visual inspection of the output images shows alignment, it is apparent that the procedure was able to successfully and accurately register the two images.

Shown in Fig. 3(e) is the result of fusing the two registered images shown in Figs. 3(c) and 3(d). The spatial resolution of the SIMS image is limited by the focus of the primary ion beam, in this case, for a C_{60} beam (about $1 \mu\text{m}$) which limits the visual quality of the image. However, the fluorescence image is limited by the magnification power of the microscope, which results in a higher resolution image. In addition, the signal intensity of the fluorescence emission of the FITC dye is higher than the secondary ion yield of the dye. After fusion of the two images, the resulting image maintains the resolution of the input fluorescence image while combining the chemical information present in the SIMS image. The letter R which appeared blurry in the SIMS image is clearly defined in the fused image. In addition, the grid lines are well defined and contrast well with the fluorescent dye in the fused image, which is an improvement over the quality of the SIMS image. Since this system is only of one component, the fluorescence dye masked in a regular pattern, the chemical information should match exactly with the fluorescence information, which is what is observed in the fused image. The resulting fused image serves as an excellent proof of concept for registering a SIMS image with a microscopy image as a preprocessing step for image fusion.

It should be noted that for this example, the surface of the sample is not flat, as the grid was mounted on top of the spin-cast fluorescent dye. This could present an issue when comparing an optical microscopy image alongside a SIMS image, as the viewing angle is not the same for each analysis method. The light source for the optical microscope is normal to the sample surface while the primary ion beam in the mass spectrometer is angled 40° off normal. Therefore, the SIMS image will exhibit shading to some degree, which would not be present in the microscope image. The degree of shading will be dependent on the relative height differences in the sample, and in the case of the copper grid, the top of the grid bars is $18 \mu\text{m}$ above the underlying film. Given that the ion beam is angled 40° off normal, this could cause pixels to be shifted up to $15 \mu\text{m}$ in both the x- and y-dimensions. This could be problematic when fusing two images, since the distributions, while registered, may not be from the same exact spatial location. However, for systems with a relatively low surface roughness, such as the RAW 264.7 cells in Sec. III C where the cell heights are 2–3 μm , this distortion will be of much less consequence.

C. Registration and fusion of optical–SIMS image pair of RAW 264.7 cells

In order to determine if the registration procedure could be used to extend the capabilities of image fusion to more

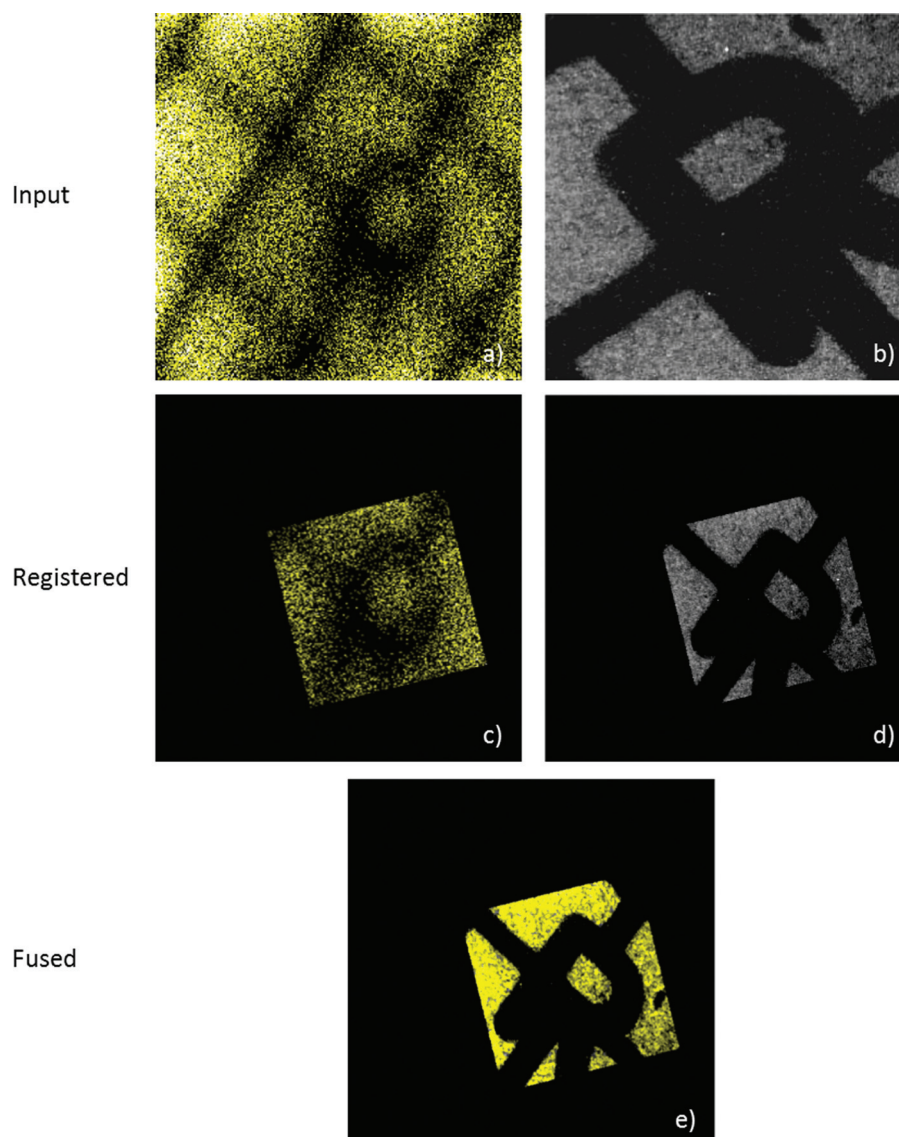


FIG. 3. Registration and fusion of fluorescence and SIMS images of FITC fluorescent dye masked by a copper mesh grid: (a) unregistered SIMS image (fixed image) of FITC $[M + H]^+$ (m/z 391) which is 256×256 pixels with a field of view of $215 \times 215 \mu\text{m}$; (b) unregistered fluorescence microscopy image (moving image) with a field of view of approximately $120 \times 120 \mu\text{m}$; (c) registered SIMS image after transformation; (d) registered fluorescence image after resampling; and (e) resulting fused image of (c) and (d).

relevant and interesting systems, a pair of images of RAW 264.7 cells was acquired. Similar to the previous example, microscopy was chosen as the high resolution data source to register and fuse with a SIMS image; however, in this case, optical microscopy was used. The optical microscope image, shown in Fig. 4(b), is able to resolve the cellular membrane and, in some of the cells, the nuclear region. However, the SIMS image shown in Fig. 4(a), which aims to map the

distribution of the membrane and nucleus, cannot resolve these two features of the cells with the same precision as the optical microscope. Therefore, image fusion is implemented to combine the chemical information of the cell membrane and nucleus with the resolving power of optical microscopy.

The optical image shows the cell membrane and the nucleus for each cell. In order to fuse the same chemical environment, the SIMS image of the tenth layer of the depth profile was chosen for the experiment. Etching away the previous nine layers removed the top of the cells which are not visible with optical microscopy, such that the nucleus was observed in a region antilocalized with, and within the confines of, the cell membrane.

As with the previous example, the optical image and the SIMS image were acquired using different modalities with different instrumentation. Thus, it is necessary to register the

TABLE II. Results describing the centered similarity transform from registering the two images in Fig. 3.

Translation	$(-74.3, 85.5)$
Rotation	-76.3°
Scale	2.02

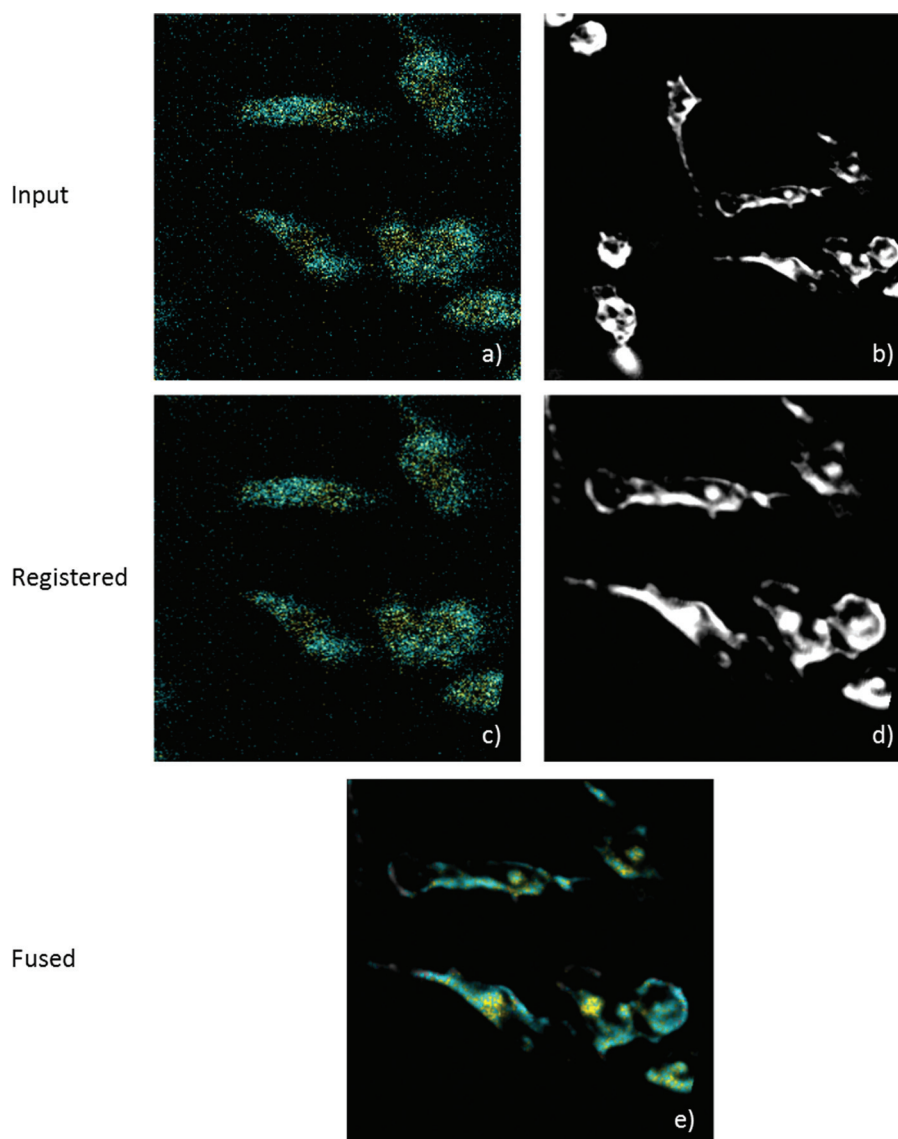


FIG. 4. Registration and fusion of optical microscopy and SIMS images RAW 264.7 cells: (a) unregistered SIMS image of phosphocholine headgroup $[\text{C}_5\text{H}_{15}\text{NPO}_4]^+$ fragment of DPPC (cyan, m/z 184.1) and adenine $[\text{M} + \text{H}]^+$ ion (yellow, m/z 136.1) which is 256×256 pixels with a field of view of $100 \times 100 \mu\text{m}$; (b) unregistered optical microscopy image with a field of view of approximately $200 \times 200 \mu\text{m}$; (c) registered SIMS image after transformation; (d) registered optical image after resampling; and (e) resulting fused image of (c) and (d).

images before performing image fusion. Again, a centered similarity transform was used to correct for the different fields of view, as well as the translation and rotation movements between the two images. To determine the transform, the total ion image from the tenth layer (not pictured; see the supplementary Fig. SI-3) of the SIMS depth profile was selected as the fixed image because it was more clear and of higher intensity than the SIMS image shown in Fig. 4(b). Since the total ion image shows brighter intensity for the substrate signal than the biological signals, the grayscale optical image was inverted to match the intensity distribution. An estimated transform was generated and passed to the registration procedure as a starting point by manually scaling, rotating, and translating the moving image with respect to the fixed image. The registered images are shown

in Figs. 4(c) and 4(d), and the transform results are shown in Table III.

The transform determined above was then applied to the two input images shown in Figs. 4(a) and 4(b) to produce the registered images shown in Figs. 4(c) and 4(d). Visual inspection shows that the two images appear to be registered very well. When comparing the resulting scale and rotation, 0.577 and -11.7° , respectively, to the estimated input

TABLE III. Results describing the centered similarity transform from registering the two images in Fig. 4.

Translation	(107, 56.4)
Rotation	-11.7°
Scale	0.577

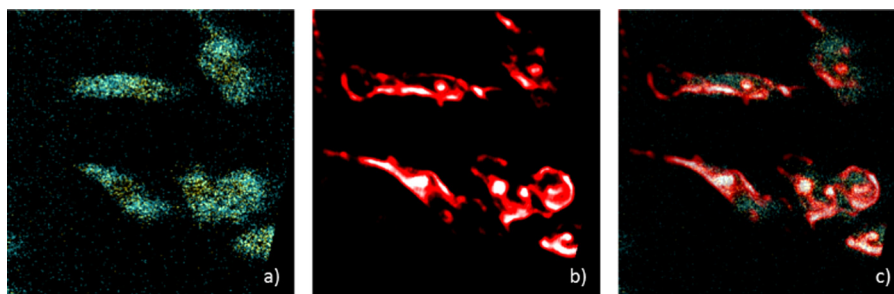


FIG. 5. Recolored optical image to show precision of the registration procedure: (a) registered SIMS image from Fig. 4(c); (b) registered optical microscopy image from Fig. 4(d) recolored with red hue to aid in visualization; and (c) overlay of images by making SIMS image 50% transparent.

transform, 0.590 and -12.8° , respectively, agreement is also observed. To visualize the success of the registration procedure, the optical image was recolored with a red hue and the SIMS image was overlaid with the recolored image, the result of which is shown in Fig. 5. By doing so, the registration of the two images becomes very clear, as the outlines and shapes of the cells match between the optical image and the SIMS image.

The final step is to fuse the registered images to combine the spatial resolution of the optical image with the chemical information of the SIMS image. The fused image is shown in Fig. 4(e) and clearly shows the distribution of the 1,2-dipalmitoyl-sn-glycero-3-phosphocholine (DPPC) signal around the cell membrane. In addition, within some of the cells, the adenine signal of the nucleus is observed in greater detail and resolution than in the input SIMS image.

While the resulting fused image shows a marked increase in resolution and image quality over the SIMS image, the spatial distribution of the nucleus for some of the cells does not appear to fall within the confines of the cell membrane. This appears most noticeably in the two cells at the left of the image. At first, it may seem that the registration procedure failed and that the distributions are shifted incorrectly. However, when looking back at the original SIMS image, it is seen that the nuclei for these two cells do not have clear, distinct distributions within the cell membrane signal. Instead, the adenine signal spreads out and overlaps with the DPPC signal around parts of the membrane. Interestingly, the adenine signal does not spread out further than the DPPC signal. All of this seems to suggest that the distribution in the x - and y -dimensions is not necessarily correct, which is likely due to the fact that a three-dimensional object is being imaged. The cells that show clear nuclei within the cell membrane are observed in the optical and SIMS images to be more spread out, which happens to some cells as they grow to replicate in a new area of the substrate. This would result in cells that are more flat, which would reduce the effects of imaging three-dimensional objects, and would explain why some cells show the distribution expected in layer ten of the depth profile and some do not. Regardless, the issue is not with the registration procedure. As shown in Fig. 5, the optical and SIMS images match up very well. In fact, the distortion of the spatial distribution of materials

observed may not have been noticed if image fusion, and thus image registration, had not been performed.

IV. SUMMARY AND CONCLUSIONS

Image registration has been implemented as a necessary preprocessing step for an image pair before performing image fusion. Successfully mapping the two input images to the same image space is essential for fusing images acquired with different modalities, especially when the two are from different instruments. Examples of image registration and fusion with SIMS and optical microscopy images demonstrated the ability of a registration procedure which implements the ITK registration framework. By successfully registering SIMS images with optical microscopy images, the applications of image fusion to SIMS expands to, conceivably, any external source of higher resolution data.

ACKNOWLEDGMENTS

The authors thankfully acknowledge financial support from the Department of Energy Grant No. DE-FG-02-06ERER15803 and the National Science Foundation Grant No. CHE 1212645.

¹A. Ashoori, B. Moshiri, and S. K. Setarehdan, *3rd International Symposium on Communications, Control and Signal Processing* (2008), Vols. 1–3, p. 20.

²J. L. Rubio-Guivernau, V. Gurchenkov, M. A. Luengo-Oroz, L. Duloquin, P. Bourguine, A. Santos, N. Peyrieras, and M. J. Ledesma-Carbayo, *Bioinformatics* **28**, 238 (2012).

³Z. Wang, D. Zhou, C. Armenakis, D. Li, and Q. Li, *IEEE Trans. Geosci. Remote Sens.* **43**, 1391 (2005).

⁴X. Huang, D. W. Wen, J. F. Xie, and L. P. Zhang, *IEEE Trans. Geosci. Remote Sens.* **11**, 753 (2014).

⁵J. Choi, K. Yu, and Y. Kim, *IEEE Trans. Geosci. Remote Sens.* **49**, 295 (2011).

⁶S. T. Li, H. T. Yin, and L. Y. Fang, *IEEE Trans. Geosci. Remote Sens.* **51**, 4779 (2013).

⁷F. Nencini, A. Garzelli, S. Baronti, and L. Alparone, *Inf. Fusion* **8**, 143 (2007).

⁸C. Pohl and J. L. van Genderen, *Int. J. Remote Sens.* **19**, 823 (1998).

⁹K. P. S. Shivsubramani Krishnamoorthy, *Int. J. Comput. Appl.* **9**, 25 (2010).

¹⁰Z. Zhong and R. S. Blum, *Proc. IEEE* **87**, 1315 (1999).

¹¹A. Henderson, J. S. Fletcher, and J. C. Vickerman, *Surf. Interface Anal.* **41**, 666 (2009).

¹²B. Tyler, G. Rayal, and D. Castner, *Biomaterials* **28**, 2412 (2007).

- ¹³B. Tyler, *Appl. Surf. Sci.* **203**, 825 (2003).
- ¹⁴B. T. Wickes, Y. Kim, and D. G. Castner, *Surf. Interface Anal.* **35**, 640 (2003).
- ¹⁵J. G. Tarolli, L. M. Jackson, and N. Winograd, *J. Am. Soc. Mass Spectrom.* **25**, 2154 (2014).
- ¹⁶J. G. Tarolli, H. Tian, and N. Winograd, *Surf. Interface Anal.* **46**, 217 (2014).
- ¹⁷T. Milillo, R. Hard, B. Yatzor, M. E. Miller, and J. Gardella, *Surf. Interface Anal.* **47**, 371 (2015).
- ¹⁸B. Zitova and J. Flusser, *Image Vision Comput.* **21**, 977 (2003).
- ¹⁹G. Pajares and J. M. de la Cruz, *Pattern Recognit.* **37**, 1855 (2004).
- ²⁰S. Klein, M. Staring, K. Murphy, M. A. Viergever, and J. P. W. Pluim, *IEEE Trans. Med. Imaging* **29**, 196 (2010).
- ²¹J. Kim and J. A. Fessler, *IEEE Trans. Med. Imaging* **23**, 1430 (2004).
- ²²K. Mori, D. Deguchi, J. Sugiyama, Y. Suenaga, J. Toriwaki, C. R. Maurer, H. Takabatake, and H. Natori, *Med. Image Anal.* **6**, 321 (2002).
- ²³D. Mattes, D. R. Haynor, H. Vesselle, T. K. Lewellen, and W. Eubank, *IEEE Trans. Med. Imaging* **22**, 120 (2003).
- ²⁴X. L. Dai and S. Khorram, *IEEE Trans. Geosci. Remote Sens.* **37**, 2351 (1999).
- ²⁵R. M. Braun, P. Blenkinsopp, S. J. Mullock, C. Corlett, K. F. Willey, J. C. Vickerman, and N. Winograd, *Rapid Commun. Mass Spectrom.* **12**, 1246 (1998).
- ²⁶T. S. Yoo, M. J. Ackerman, W. E. Lorensen, W. Schroeder, V. Chalana, S. Aylward, D. Metaxas, and R. Whitaker, *Stud. Health Technol.* **85**, 586 (2002).
- ²⁷H. J. Johnson, M. McCormick, and L. Ibanez *The ITK Software Guide*, 3rd ed. (Kitware Inc., 2013).
- ²⁸J. P. W. Pluim, J. B. A. Maintz, and M. A. Viergever, *IEEE Trans. Med. Imaging* **22**, 986 (2003).
- ²⁹See supplementary material at <http://dx.doi.org/10.1116/1.4939892> for additional proof of concept experiments and additional images used for the registration of images in Fig. 4.